DO-TH 00/04
March 2000

Fragmentation Functions from Flavour-inclusive and Flavour-tagged e^+e^- Annihilations

S. Kretzer

Institut für Physik, Universität Dortmund
D-44221 Dortmund, Germany

Abstract

Fitting Z^0-pole data from ALEPH and SLD, and TPC data at a lower c.m.s. energy, we fix the boundary condition for NLO parton→hadron (hadron= $\pi^\pm, K^\pm, \sum_h h^\pm$) fragmentation functions (FFs) at the low resolution scale of the radiative parton model of Glück, Reya and Vogt (GRV). Perturbative LO↔NLO stability is investigated. The emphasis of the fit is on information on the fragmentation process for individual light (u, d, s) and heavy (c, b) quark flavours where we comment on the factorization scheme for heavy quarks in e^+e^- annihilations as compared to deep inelastic production. Inasmuch as the light quark input parameters are not yet completely pinned down by measurements we assume power laws to implement a physical hierarchy among the FFs respecting valence enhancement and strangeness suppression both of which are manifest from recent leading particle measurements. Through the second Mellin moments of the input functions we discuss the energy-momentum sum rule for massless FFs. We discuss our results in comparison to previous fits and recent 3-jet measurements and formulate present uncertainties in our knowledge of the individual FFs.

1 Introduction

In this article we consider the production of identified light hadrons in e^+e^- collisions or more precisely the production of charged hadrons built from light up, down and strange valence quarks, i.e. dominantly pions, kaons and nucleons. Within perturbative QCD the light hadron production dynamics of e^+e^- annihilations inevitably comprise a nonperturbative long distance component from the nonperturbative hadronization of perturbatively produced partons. We will fix this latter nonperturbative component in the canonical QCD framework of parton→hadron fragmentation functions (FFs) at the low resolution input scale of the radiative GRV parton model [1]. In the naive parton model the FF $D_p^h(z)$ has the interpretation of a probability density that some final state parton p hadronizes (or *fragments*) into a mean number $D_p^h(z)dz$ of hadrons h per dz where z is the fractional momentum which h receives from the parton. Field and Feynman have constructed [2] an early set of mesonic fragmentation functions footing solely on this intuitive probabilistic interpretation. Today's state of the art embeds the $D_p^h(z)$ functions in the framework of QCD factorization theory [3] including explicit operator definitions [4]. Fragmentation functions are the final state analogues of the initial state parton distribution functions (PDFs) and precisely as the PDFs do the FFs parametrize our ignorance of QCD bound state dynamics. Fragmentation functions into identified hadrons are therefore in their own right an interesting source of information on the hadronization process and they are a necessary ingredient to interpret present and future measurements of any one-particle-inclusive hard cross section within fundamental (perturbative) QCD theory as compared to Monte Carlo model approaches. Whereas PDFs are mainly determined from fully inclusive DIS the cleanest extraction of FFs is from e^+e^- collisions. FFs pinned down in e^+e^- can, by universality, then be applied to, e.g., the hadro- or leptoproduction of identified hadrons and compatibility with the transverse momentum spectrum produced in photon-proton collisions was found in [5]. From a combined use of both - fragmentation *and* parton distribution functions - in one hadron inclusive deep inelastic scattering information on the initial state parton flavour can be obtained from leading particle ef-

fects where a high energetic hadron inside a jet remembers the valence parton it has been produced off [6–8]. Parton information from semi-inclusive measurements based on an understanding of the fragmentation process also extends to polarized DIS where the spin flavour structure of the nucleon sea is still rather unknown [6, 9]. In this article we will restrict ourselves to the defining e^+e^- process and leave other applications to future work [10].

The recent years have seen much effort [5, 11–18] to establish a similar technical skill for FFs as for existing sets of PDFs [1, 19, 20]. We will take a further step towards this goal and for this purpose we concentrate mainly on data which constrain the flavour decomposition of fragmentation spectra; such data sets exist at the Z^0 pole for charged $\pi^\pm$ and $K^\pm$ mesons from SLD [21] and for the inclusive sum over charged hadrons from ALEPH [17]. Lower energy counterparts from TPC [22] will be included to correctly take QCD scaling violations - which have been re-established recently in [5, 13, 17] - into account. The flavour separation confronts us with the question of how to treat heavy flavours within e^+e^- production dynamics which we will answer in some detail. Especially the SLD data sets on flavour tagged fragmentation into $\pi^\pm$ and $K^\pm$ mesons contain new flavour information not included in previous fits [5] to which we compare our results, thereby formulating the present uncertainty of our knowledge on the individual FFs.

2 Parton Fragmentation in e^+e^- Collisions Beyond the Leading Order

The NLO framework[1] for one-hadron-inclusive e^+e^- annihilations is well known since long [5, 11, 13, 16, 23–27] and we restrict ourselves to a brief theoretical introduction here in which we closely follow Ref. [11] in notation.

[1]The formulae below include the LO framework in an obvious way by dropping subleading terms.

To be specific we will consider the reaction

$$\frac{d\sigma^{(e^+e^-\to\gamma,Z^0\to hX)}}{dz} \equiv \frac{d\sigma^h}{dz} = \frac{d\sigma^h_T}{dz} + \frac{d\sigma^h_L}{dz} \quad , \tag{1}$$

where

$$z \equiv 2E_h/Q = 2P_h \cdot q/Q^2 \tag{2}$$

is the energy[2] E_h of the observed hadron scaled to the beam energy $Q/2 \equiv \sqrt{s}/2$;[3] with the positron/electron beam momentum $P_{e^\pm} = (Q/2, 0, 0, \pm Q/2)$ and $q = P_{e^+} + P_{e^-}$. The r.h.s. of Eq. (1) distinguishes the contributions from transverse (T) and longitudinal (L) virtual bosons, where the polarization axis is in the direction of the momentum of the observed hadron h. Experimental data are commonly not presented for the absolute cross section in Eq. (1) but for the normalized distribution

$$\frac{1}{N_{tot}} \frac{\Delta N^h}{\Delta z} \to \frac{1}{\sigma_{tot}} \frac{d\sigma^h}{dz} \quad ; \text{ as } \Delta z \to 0 \quad , \tag{3}$$

where ΔN^h counts the registered h-events per bin Δz and N_{tot} denotes the inclusive sum of hadronic events. Within perturbative QCD and up to $\mathcal{O}(\alpha_s^1)$ the total hadronic cross section σ_{tot} is given by

$$\sigma_{tot} = \sum_q \sigma_0^q(s) \left[\left(1 + \frac{\alpha_s(Q^2)}{\pi} \right) + \mathcal{O}\left(\frac{m_q^2}{Q^2} \right) \right] + \mathcal{O}\left(\frac{\Lambda^4_{QCD}}{Q^4} \right) \tag{4}$$

where the parton model, i.e. $\mathcal{O}(\alpha_s^0)$, electroweak cross sections σ_0^q for producing a $q\bar{q}$ pair are given in the Appendix. The power suppressed terms arise from perturbative quark mass effects $[\mathcal{O}(m_q^2/Q^2)]$ or nonperturbative higher operator matrix elements $[\mathcal{O}(\Lambda^4_{QCD}/Q^4)]$. We will discuss the quark mass effects in Section 4 where we give ample reasons for our choice of the factorization scheme. Higher operators are not considered in this article.

[2] In cases where experimental data are presented in the *momentum* scaling variable $z_p \equiv 2p_h/Q$ we will transform the data to z using the relativistic energy momentum relation $E_h^2 = p_h^2 + m_h^2$ and *assuming* pion production dominance ($m_h = m_\pi$) whenever the hadron h is not specified.

[3] Though $s \equiv Q^2$ we will use both variables - s and Q^2 - in the following in their rôle as the c.m.s. energy and perturbative hard scale, respectively.

QCD factorization theory predicts that

$$\frac{d\sigma^h_{P=T,L}}{dz} = \sum_{i=\left\{\begin{array}{l} q=u,d,s,\ldots \\ \bar{q}=\bar{u},\bar{d},\bar{s},\ldots \\ g \end{array}\right.} \left[\int_z^1 \frac{d\zeta}{\zeta} C_P^i\left(\zeta, Q^2, \mu^2_{F,R}\right) D_i^h\left(\frac{z}{\zeta}, \mu_F^2\right) + \mathcal{O}\left(\frac{m_q^2}{Q^2}\right)\right] + \mathcal{O}\left(\frac{\Lambda^n_{QCD}}{Q^n}\right) \tag{5}$$

where the power n of the nonperturbative corrections [28] cannot be determined from an operator product expansion based analysis, contrary to $n = 4$ in Eq. (4) and to deep inelastic scattering where higher twists are known to be suppressed by a power $n = 2$. As anywhere $\mu^2_{F,R}$ are the factorization and renormalization scale, respectively, and we will set them both equal to $\mu^2 \equiv \mu^2_{F,R} = Q^2$ in the applications. The treatment of charm and bottom in the sum over quark flavours $q = u, d, s, ...$ in (5) will be discussed in Section 4. The coefficient functions C_P^i are given up to $\mathcal{O}(\alpha_s^1)$ in the $\overline{\rm MS}$ scheme [11, 23, 24] by

$$\begin{aligned}
C_T^q\left(\zeta, Q^2, \mu^2_{F,R}\right) &= \left[\delta(1-\zeta) + \frac{\alpha_s(\mu_R^2)}{2\pi}\, C_F\, c_T^q\left(\zeta, \frac{Q^2}{\mu_F^2}\right)\right] \sigma_0^q(s) \\
C_T^g\left(\zeta, Q^2, \mu^2_{F,R}\right) &= \frac{\alpha_s(\mu_R^2)}{2\pi}\, C_F\, c_T^g\left(\zeta, \frac{Q^2}{\mu_F^2}\right) \sum_q \sigma_0^q(s) \\
C_L^q\left(\zeta, Q^2, \mu^2_{F,R}\right) &= \frac{\alpha_s(\mu_R^2)}{2\pi}\, C_F\, c_L^q\left(\zeta, \frac{Q^2}{\mu_F^2}\right) \sigma_0^q(s) \\
C_L^g\left(\zeta, Q^2, \mu^2_{F,R}\right) &= \frac{\alpha_s(\mu_R^2)}{2\pi}\, C_F\, c_L^g\left(\zeta, \frac{Q^2}{\mu_F^2}\right) \sum_q \sigma_0^q(s)
\end{aligned} \tag{6}$$

and for antiquarks $C^{\bar{q}}_{T,L} = C^q_{T,L}$. The $c^{q,g}_{T,L}$ and σ_0^q can be found in the Appendix. The $\mathcal{O}(\alpha_s^2)$ contributions to the coefficient functions $C^{q,g}_{T,L}$ in (6) are known [29] but are of next-to-next-to-leading order and will therefore not be considered in this NLO analysis, with one exception to be discussed in Section 3.

In the $\overline{\rm MS}$ scheme the parton model expectation

$$\int_0^1 dz\; z \sum_h D_i^h(z) = 1 \tag{7}$$

that the entire parton energy is shared by the parton's fragmentation products is preserved under renormalization $[D_i^h(z) \to D_i^h(z, \mu^2)]$ of the fragmentation functions by energy

conservation

$$\frac{1}{2\sigma_{tot}} \int_0^1 dz\ z \sum_h \frac{d\sigma^h}{dz} = 1 \tag{8}$$

where $d\sigma^h$ is related to the D_i^h via Eqs. (1), (5). The renormalized fragmentation functions D_i^h obey massless Altarelli-Parisi-type renormalization group equations

$$\frac{\partial D_j^h(z,Q^2)}{\partial \ln Q^2} = \sum_i \int_z^1 \frac{d\zeta}{\zeta}\ P_{ij}\left(\frac{z}{\zeta}, Q^2\right) D_i^h(\zeta, Q^2) \tag{9}$$

where the P_{ij} have a perturbative expansion

$$P_{ij}(z,Q^2) = \frac{\alpha_s(Q^2)}{2\pi}\ P_{ij}^{(0)}(z)\ +\ \left(\frac{\alpha_s(Q^2)}{2\pi}\right)^2\ P_{ij}^{(1)}(z)\ +\ \mathcal{O}\left(\alpha_s^3\right) \quad . \tag{10}$$

The NLO pieces $P_{ij}^{(1)}$ of the timelike P_{ij} in (10) differ from their spacelike counterparts. The P_{ij} are implicitly understood to represent the *timelike* splitting functions in [25][4].

The evolution equations will be solved analytically in Mellin n-space as described, e.g. in [24, 26]. We have included the n-space expressions [24, 26] for the $c_{L,T}^{q,g}$ in Eq. (6) in the Appendix. The timelike splitting functions (10) up to two loop order [25] have been transformed to n-space in [26]. To keep this article compact we do not reproduce these lengthy formulae nor do we repeat the solution of Eq. (9) in Mellin space. Suffice to say here that some functional input forms for the $D_i^h(z,\mu^2)$ are required where we make the Ansatz

$$D_i^h(z,\mu_0^2) = N_i\ z^{\alpha_i^h}\ (1-z)^{\beta_i^h} \tag{11}$$

which we assume to hold for light partons ($i = g, u, d, s$ and corresponding antiquarks) at the low input scale $\mu_0^2 = 0.4$ GeV^2 of the recent NLO revision [1] of the radiative parton model [30–33]. (Accordingly, $\mu_0^2 = 0.26$ GeV^2 [1] will serve as the input scale for the LO fits to be discussed below.) As already mentioned, the treatment of heavy flavours will be specified in the next Section. Along with the low input scale μ_0^2 we also adopt the evaluation of α_s^{NLO} used in [1], i.e. we numerically solve the renormalization group equation

$$\frac{d\alpha_s(Q^2)}{d\ln Q^2} = -\frac{\beta_0}{4\pi}\ \alpha_s^2(Q^2) - \frac{\beta_1}{16\pi^2}\ \alpha_s^3(Q^2) \tag{12}$$

[4] A misprint in the second Ref. of [25] was corrected in [26, 27].

exactly by finding the root of

$$\ln \frac{Q^2}{\Lambda_f^2} = \frac{4\pi}{\beta_0 \alpha_s(Q^2)} - \frac{\beta_1}{\beta_0^2} \ln \left[\frac{4\pi}{\beta_0 \alpha_s(Q^2)} + \frac{\beta_1}{\beta_0^2} \right] \tag{13}$$

with $\beta_0 = 11 - 2f/3$ and $\beta_1 = 102 - 38f/3$ and where the number f of active flavours in the quark loop contributions to the beta function is

$$f = \begin{cases} 3, \mu_0^2 < Q^2 < m_c^2 \\ 4, m_c^2 < Q^2 < m_b^2 \\ 5, m_b^2 < Q^2 < m_t^2 \\ 6, m_t^2 < Q^2 \end{cases} \tag{14}$$

with [1] $m_{c,b,t} = 1.4,\ 4.5,\ 175$ GeV. Eq. (14) guarantees the continuity of α_s at the transition scales $m_{c,b,t}$ in the $\overline{\rm MS}$ scheme up to two loops [34], if we furthermore adopt [1] $\Lambda_{3,4,5,6} = 299.4,\ 246,\ 167.7,\ 67.8$ MeV in NLO (and $\Lambda_{3,4,5,6} = 204,\ 175,\ 132,\ 66.5$ MeV in LO). The continuity of α_s at the transition scales Q_0, where $f \to f+1$, is guaranteed for $Q_0^2 = m_{c,b,t}^2$ [34] from the ratio of the renormalization constants Z_3 in a renormalization scheme with f and $f+1$ active flavours, respectively. Hence the continuity is not affected by the choice of solving the NLO renormalization group equation exactly as implied by Eq. (13) or by an analytical approximation up to some inverse power of $\ln Q^2$, as, e.g., in Eq. (9.5a) of [35]. The exact numerical solution of Eq. (13) is more appropriate [1] in the low $Q^2 \lesssim m_c^2$ regime and will be used over the entire Q^2 range.

3 The Longitudinal Cross Section $d\sigma_L^h/dz$

We shall comment here briefly on the counting of perturbative orders for the longitudinal structure function on the r.h.s. of (1). Experimentally $d\sigma_L^h/dz$ is extracted [17] by reweighting inclusive hadronic events according to their polar angle (θ) distribution as

$$\frac{d\sigma_L^h}{dz} = \int_{-v}^{v} d\cos\theta \ \frac{d^2\sigma^h}{dz d\cos\theta} \ W_L(\cos\theta, v) \quad , \tag{15}$$

where the projector W_L was introduced in [11] and $v = |\cos\theta|_{\rm max}$ is set by the detector geometry, e.g. $v = 0.94$ for ALEPH [17].

From the theoretical side we can read off Eqs. (5), (6) that $d\sigma_L^h/dz$ receives its leading *nonzero* (finite and scheme-independent) contribution at $\mathcal{O}(\alpha_s^1)$. When considering data on $d\sigma_L^h$ obtained from reweighted events as in (15) we will therefore include for our *next-to-leading order* analysis the $\mathcal{O}(\alpha_s^2)$ contributions of Ref. [29]. We will, however, treat the $\mathcal{O}(\alpha_s^1)$ coefficients $C_L^{q,g}$ in (6) as *subleading* (NLO) contributions to the *total* $d\sigma^h = d\sigma_T^h + d\sigma_L^h$ in Eq. (1) which receives its *leading* contribution from the $d\sigma_T^h$ component to $\mathcal{O}(\alpha_s^0)$.

To $\mathcal{O}(\alpha_s^2)$ the convolutions in (5) are most conveniently decomposed according to the flavour group as described in [29]. The corresponding coefficient functions for $d\sigma_L^h/dz$ are given in Eq. (17), (18) and (20) in the second Ref. of [29]. For the transformation to Mellin n space the nontrivial ones of the required identities can be found in [36–38].

4 Treatment of Heavy Flavours

Heavy quark initiated jets provide a substantial contribution to one-hadron-inclusive e^+e^- annihilation spectra. In principle, the hard scattering production of heavy quarks has a well defined and unique perturbative expansion within QCD but the residual freedom of arranging the perturbation series at finite order leads into scheme ambiguities [39]. The key question is whether the convergence of perturbative calculations improves if fixed order calculations are supplied with an additional resummation of quasi-collinear logarithms $[(\alpha_s/2\pi)\ln(Q^2/m^2)]^n$ to all orders n, where m is the heavy quark mass. The explicit all order resummation is equivalent to solving massless evolution equations from an input scale of $\mathcal{O}(m)$. The boundary condition at the input scale is again calculable at fixed order and has been derived for e^+e^- annihilations in [40] to $\mathcal{O}(\alpha_s)$.

Fixed NLO calculations seem at present to be reliable [1, 41] for the deep inelastic production of charm and bottom - dominantly in scattering events off wee gluons at low partonic c.m.s. energy where mass effects are most important [41]. Contrarily, in e^+e^- an-

nihilations each quark of a primary heavy quark pair receives the energy $Q/2 \gg m$ at the intermediate boson decay vertex. Such a highly relativistic quark will obviously not 'feel' its mass anymore and at the energies which we will consider, primary up- and down-type quarks[5] are each produced in equal number, irrespective of the quark mass. We therefore expect heavy quarks in e^+e^- to behave essentially like massless partons with mass (quasi-)singularities to be resummed. In [42–44] all order NLO collinear resummations were demonstrated to be required and adequate in order to describe the energy distribution of charm and bottom quarks over the partonic final state of high energy e^+e^- annihilations. In particular, all order massless resummations for charm quarks were proven to be necessary to describe the amount of secondary charm quarks from $g \to c\bar{c}$ splittings in the parton showering, visible in a rise of the cross section at lower z as observed by OPAL [45] and ALEPH [46] and as opposed to the fixed $\mathcal{O}(\alpha_s^2)$ order contribution $Z^0 \to q\bar{q}g \to q\bar{q}c\bar{c}$ [47] which turns out to be far too small [43, 44]. Bottom production has an evolution length which is shorter by the amount of $\Delta \ln Q^2 = \ln(m_b^2/m_c^2)$ which suffices to suppress secondary bottom pairs as experimentally observed [48] in a flat $z \to 0$ B-spectrum.

Hence, we will include $q_{_H} \to h$ FFs mixing under evolution with their light parton analogues, i.e. describing all long distance (collinear parton showering *and* hadronization) effects of the fragmentation process. Heavy flavours are treated above their respective $\overline{\rm MS}$ 'thresholds' $Q_0 = m_{c,b}$ as active flavours in the evolution of the $D^h_{q,g}(z,\mu^2)$ in Eq. (9). We adopt the functional form of Eq. (11) also for $D^h_{c,b}$, i.e.

$$D^h_{i=c,b}(z,\mu_i^2) = N_i \; z^{\alpha_i^h} \; (1-z)^{\beta_i^h} \quad , \tag{16}$$

to hold at $\mu_i^2 = m_i^2$ along Eq. (14) which guarantees the continuity of α_s at μ_i^2 in NLO. The $D^h_{i=c,b}$ are then *dis*continuously 'switched on' in the evolution at m_i^2 but enter the cross section in Eq. (1) only above the partonic threshold $Q^2 > 4m_i^2$.[6] It is certainly questionable [13] to fit pure QCD fragmentation functions for heavy quarks to inclusive

[5] We do, of course, not consider the superheavy top quark here.

[6] The partonic threshold $4m_i^2$ - or similar low resonance threshold scales [5] - may therefore be considered a natural choice for μ_i^2. We follow existing PDF sets which avoid the discontinuities in α_s induced by $\mu_i \neq m_i$.

or heavy quark tagged data because charm and bottom jets are highly contaminated by weak decay channels. Adopting such a procedure anyway is a necessity as long as data corrected for weak decays do not exist.

5 Fitting Procedure

Early model attempts [49] to generate fragmentation functions entirely by QCD dynamics from a delta peak input $D_p^h(z) \propto \delta(1-z)$ are outruled by modern high statistics data [17, 21, 22] which require smooth input functions (11), (16) to be fitted to experiment. Recently, fragmentation functions have been fitted to e^+e^- production data using either free fit Ansätze [5] or Ansätze strongly constrained by $\mathrm{SU(3)_f}$ symmetry [15]. We will take an intermediate path and constrain free fit Ansätze by making power law assumptions about valence enhancement and strangeness suppression within the radiative parton model of Refs. [1, 30–33]. The model is originally tailored for parton distribution functions to perturbatively generate the high population of quarks and gluons in hadrons at low Bjorken x. It should be clear from the scratch that its predictivity cannot be transfered to FFs where a well defined *low* z analogue of the deep inelastic *low* x regime is missing [16].

Our aim is to pin down fragmentation functions $D_i^h(z,\mu^2)$ for (anti-)quarks and gluons hadronizing into charged pions ($h = \pi^+, \pi^- \equiv \pi^{+,-}$), charged kaons ($h = K^+, K^- \equiv K^{+,-}$) and the inclusive sum over charged hadrons [$\sum_h (h^+ + h^-) \equiv \sum h^{\pm}$];[7] basically from high statistics data at the Z^0 peak measured by ALEPH [17] at LEP ($\sum h^{\pm}$) and by SLD [21] ($\pi^{\pm}, K^{\pm}$) at SLAC. Besides their high statistical accuracy, these data sets have the advantage of furnishing along with their fully inclusive measurements also flavour enriched events which can be used to fix the flavour structure of the $D_i^h(z,\mu^2)$ to some extent. Both data sets distinguish between light quark (u, d, s), charm, and bottom events where the quark flavour refers to the primary Z^0-boson decay vertex. Since pure flavour

[7] Similarly, $\pi^{\pm}$ will denote $\pi^+ + \pi^-$ to be distinguished from $\pi^{+,-} \equiv \pi^+, \pi^-$; for kaons accordingly.

separated sets cannot be obtained directly [17, 21], Monte Carlo simulations are required to estimate the flavour composition of the tagged data sets. From these Monte Carlo studies the flavour enriched event samples have been unfolded at a given systematic uncertainty to pure flavour sets for the SLD data whereas ALEPH quotes percentages for each flavour contribution to any of its flavour enriched samples. In the latter case some uncertainty will reside in the translation of the Monte Carlo studies to the perturbative calculations we are performing here which can unfortunately not be quantified since no systematic errors are quoted [17] for the percentages. Anyway, we will reweight the electroweak couplings in Table 3 in the Appendix to reproduce the ALEPH flavour composition as quoted in [17]. In order to have our FFs respect QCD scaling violations properly we include lower scale ($\sqrt{s} = 29$ GeV) TPC data [22] in our fits which also furnish flavour information (unfolded to pure $\{u, d, s\}$, c and b event samples) for $\sum h^{\pm}$ and for $\pi^{\pm}$ but only inclusive measurements for $K^{\pm}$. Needless to say, the fits will be dominated statistically by the Z^0-pole measurements of ALEPH and SLD.

Our Ansätze for the fragmentation functions will be the ones of Eqs. (11), (16) for light parton and heavy quark fragmentation, respectively, where we assume the following symmetries and hierarchy

$$D_q^{h^+,h^-} = D_{\bar{q}}^{h^-,h^+}; \quad h = \pi, K \tag{17}$$

$$D_d^{\pi^+} = D_{s,\bar{s}}^{\pi^+} < D_u^{\pi^+} = D_{\bar{d}}^{\pi^+} \tag{18}$$

$$D_{\bar{u}}^{K^+} = D_{d,\bar{d}}^{K^+} < D_u^{K^+} < D_{\bar{s}}^{K^+} \quad , \tag{19}$$

where Eq. (17) respects charge conjugation and Eqs. (18), (19) should hold from the valence structure of pions and kaons and strangeness suppression. The equality in Eq. (18) seems to be confirmed by 'leading particle' measurements [50] which also indicate the second *in*equality in Eq. (19) at large z from the suppression of secondary $s\bar{s}$ formation which is required to form a K^+ from a u but not from an $\bar{s}$ quark. Beyond strangeness suppression, in $\pi^{+,-}$ or $K^{+,-}$ production we expect differences from favoured valence-type (e.g. $u \to \pi^+$) and unfavoured sea-type (e.g. $s \to \pi^+$) fragmentation channels. Nevertheless, we assume a universal $z \to 0$ behaviour, determined by the input parameters

N_i and α_i in (11), This assumption is guided by the idea that the valence enhancement of, say, $u \to \pi^+$ fragmentation should manifest itself mainly as a 'leading particle effect' [50], parametrized by β_i in (11) as $z \to 1$. We will *assume* [51]

$$\beta_d^{\pi^+} = \beta_{s,\bar{s}}^{\pi^+} = \beta_{u,\bar{d}}^{\pi^+} + 1 \quad , \quad \beta_{\bar{u}}^{K^+} = \beta_{d,\bar{d}}^{K^+} = \beta_u^{K^+} + 1 = \beta_{\bar{s}}^{K^+} + 2 \quad , \tag{20}$$

which suppresses $s\bar{s}$ formation as well as sea-type fragmentation as $z \to 1$. A linear suppression factor $D_d^{\pi^+}/D_u^{\pi^+} = (1-z)$ for sea-type fragmentation is compatible with semi-inclusive deep inelastic measurements [6, 8] in the range $0.1 < z \lesssim 0.8$. These measurements seem to prefer a factor $\sim (c-z)$ with $c \simeq 0.25$ for $z > 0.8$. The very large z behaviour of the $D_i^h(z)$ is, however, not very well constrained by e^+e^- measurements and from the theoretical side soft gluon resummations may become necessary [18]. Also, the universality, i.e. process-independence of the FFs in e^+e^- annihilations and semi-inclusive DIS[10], respectively, is not yet well settled at large z [8]. We therefore keep $D_d^{\pi^+}/D_u^{\pi^+} = (1-z)$ for the time being. Our assumptions in Eq. (20) are compatible with $D_d^{\pi^+}(n=2) \simeq 0.6\ D_u^{\pi^+}(n=2)$ where the second moments are defined below in Eq. (24) and where their ratio can be estimated from EMC one-pion-inclusive data [7]. These data have been analyzed in a parton model context and the extracted scale-independent FFs of [7] can therefore not be compared to our fit in more detail. The corresponding one-kaon-inclusive measurements in [7] seem to prefer an even stronger suppression of sea-type fragmentation in kaon formation. For the time being, we do, however, assume the suppression of sea-type channels to be a universal phenomenon modeled by one extra power in $(1-z)$ for the input FFs. This assumption, as any of our above assumptions on the light flavour structure of annihilation data, must obviously be expected to be violated to some extent if dedicated measurements will become possible.

If we furthermore assume for simplicity

$$D_{c,b}^{h^+} = D_{c,b}^{h^-} \tag{21}$$

to hold in the heavy quark sector[8], we are left with the following set of independent input

[8] We would expect Eq. (21) to hold exactly if heavy quark jets were not contaminated by weak decays.

parametrizations for pions and kaons:

$$\begin{aligned}
D_{u,\bar{d}}^{\pi^+}(z,\mu_0^2) &= N_u^{\pi^+} z^{\alpha_u^{\pi^+}} (1-z)^{\beta_u^{\pi^+}} \\
D_{s,\bar{s}}^{\pi^+}(z,\mu_0^2) &= N_u^{\pi^+} z^{\alpha_u^{\pi^+}} (1-z)^{\beta_u^{\pi^+}+1} \\
D_g^{\pi^+}(z,\mu_0^2) &= N_g^{\pi^+} z^{\alpha_g^{\pi^+}} (1-z)^{\beta_g^{\pi^+}} \\
D_{c,\bar{c}}^{\pi^+}(z,m_c^2) &= N_c^{\pi^+} z^{\alpha_c^{\pi^+}} (1-z)^{\beta_c^{\pi^+}} \\
D_{b,\bar{b}}^{\pi^+}(z,m_b^2) &= N_b^{\pi^+} z^{\alpha_b^{\pi^+}} (1-z)^{\beta_b^{\pi^+}}
\end{aligned} \tag{22}$$

$$\begin{aligned}
D_{\bar{s}}^{K^+}(z,\mu_0^2) &= N_{\bar{s}}^{K^+} z^{\alpha_{\bar{s}}^{K^+}} (1-z)^{\beta_{\bar{s}}^{K^+}} \\
D_u^{K^+}(z,\mu_0^2) &= N_{\bar{s}}^{K^+} z^{\alpha_{\bar{s}}^{K^+}} (1-z)^{\beta_{\bar{s}}^{K^+}+1} \\
D_{d,\bar{d}}^{K^+}(z,\mu_0^2) &= N_{\bar{s}}^{K^+} z^{\alpha_{\bar{s}}^{K^+}} (1-z)^{\beta_{\bar{s}}^{K^+}+2} \\
D_g^{K^+}(z,\mu_0^2) &= N_g^{K^+} z^{\alpha_g^{K^+}} (1-z)^{\beta_g^{K^+}} \\
D_{c,\bar{c}}^{K^+}(z,m_c^2) &= N_c^{K^+} z^{\alpha_c^{K^+}} (1-z)^{\beta_c^{K^+}} \\
D_{b,\bar{b}}^{K^+}(z,m_b^2) &= N_b^{K^+} z^{\alpha_b^{K^+}} (1-z)^{\beta_b^{K^+}} \quad .
\end{aligned} \tag{23}$$

In practice, we will express the normalizations N_i^h through the physically more interesting contributions to the energy integral in Eq. (7), given by the second Mellin moment

$$D_i^h(n=2,\mu^2) \equiv \int_0^1 dz\ z D_i^h(z,\mu^2) \tag{24}$$

which would be an exact invariant under evolution in μ^2 only if $D_i^h(n=2,\mu^2)$ were the same for all i – which is not the case. Anyway, guided by the idea of having an intermediate gluon in the parton cascade connecting a valence- and a sea-type quark we will reduce the parameter space $\{N_i^{\pi^+,-,K^+,-},\ \alpha_i^{\pi^+,-,K^+,-},\ \beta_i^{\pi^+,-,K^+,-}\}$ somewhat by demanding[9]

$$\begin{aligned}
D_g^{\pi^+}(n=2,\mu_0^2) &= \tfrac{1}{2}\left[D_s^{\pi^+}(n=2,\mu_0^2) + D_u^{\pi^+}(n=2,\mu_0^2)\right] \\
D_g^{K^+}(n=2,\mu_0^2) &= \tfrac{1}{2}\left[D_d^{K^+}(n=2,\mu_0^2) + D_u^{K^+}(n=2,\mu_0^2)\right]
\end{aligned} \tag{25}$$

which reduces the strength of the evolution of the $D_i^h(n=2,\mu^2)$ considerably and does not influence the quality of the fits.

[9] We do not include $D_{\bar{s}}^{K^+}$ in the second average of Eq. (25) because gluon fragmentation into a K^+ must be strangeness-suppressed.

Samples of inclusive charged hadrons $\sum h^\pm$ are dominated by charged pions and adding a kaon background is a reasonable approximation for most applications:

$$D_i^{\Sigma h^\pm} \simeq D_i^{\pi^\pm + K^\pm} \quad . \tag{26}$$

Eq. (26) is, however, not adequate to compare with high statistics measurement from the Z^0-pole [17], which are sensitive at the $\mathcal{O}(1\%)$-level. We will fit a small residue from higher mesons and baryons along

$$D_i^{\Sigma h^\pm} = D_i^{\pi^\pm + K^\pm} + D_i^{\text{res.}} \quad , \tag{27}$$

using again simple Ansätze as in (11), (16) where we distinguish between light flavours ($D_u^{\text{res.}} = D_d^{\text{res.}} = D_s^{\text{res.}}$), heavy charm and bottom quarks ($D_c^{\text{res.}}, D_b^{\text{res.}}$) and gluons ($D_g^{\text{res.}}$) and where $D_i^{\text{res.}} > 0$ serves as a consistency check. The residual functions amount to a sufficiently small correction not to constrain them any further. For the same reason the approximation that the hadronic residue is half positively, half negatively charged for any parton, i.e. $D_i^{\Sigma h^{+,-}} = D_i^{\pi^{+,-} + K^{+,-}} + D_i^{\text{res.}}/2$ can be safely used for the inclusive sum of only positively (negatively) charged hadrons. Altogether, the Ansätze (22)-(23), (27) with the constraints (25) will be fed into the evolution equation (9) to evaluate the cross section (1) using the factorization theorem (5). The χ^2-minimization algorithm `MINUIT` [52] will be used to obtain best possible agreement of the outcome with experimental data [17, 21, 22] over the range $0.05 < z < 0.8$. Towards low z the TPC data for charged pion production [22] at $\sqrt{s} = 29$ GeV lie above the corresponding SLD data [21] at $\sqrt{s} = M_Z$ ($d\sigma^{\text{TPC}}\big|_{z \lesssim 0.1} > d\sigma^{\text{SLD}}\big|_{z \lesssim 0.1}$) which contradicts the established [5, 17] QCD evolution ($d\sigma^{\text{QCD}}/ds\big|_{z \lesssim 0.1} > 0$) predicting that $d\sigma$ *increases* with $\sqrt{s}$ at low z. Since the SLD measurements are compatible with the LEP data of e.g. ALEPH [17] we exclude TPC charged pion data below $z < 0.1$. Data on the longitudinal structure function $d\sigma_L^{\Sigma h^\pm}$ available from ALEPH [17] will be considered for consistency but are not weighted in the fit because we found no significant statistical impact of these data on the fit results. Although one might hope $d\sigma_L$ to constrain the gluon fragmentation function because the gluon enters at 'leading' $\mathcal{O}(\alpha_s^1)$ a closer NLO inspection [53] reveals that $d\sigma_L$ is dominated by quark fragmentation over most of the z range.

$D_i^h(z,Q_0^2)$	$N_i^h\ z^{\alpha_i^h}\ (1-z)^{\beta_i^h}$	$D_i^h(n=2,Q_0^2)$
$D_{u,\bar{d}}^{\pi^+}(z,\mu_0^2)$	$N_u^{\pi^+} z^{-0.829}(1-z)^{0.949}$	0.264
$D_{s,\bar{s}}^{\pi^+}(z,\mu_0^2)$	$N_u^{\pi^+} z^{-0.829}(1-z)^{1.949}$	0.165
$D_g^{\pi^+}(z,\mu_0^2)$	$N_g^{\pi^+} z^{4.374}(1-z)^{9.778}$	0.215
$D_{c,\bar{c}}^{\pi^+}(z,m_c^2)$	$N_c^{\pi^+} z^{-0.302}(1-z)^{5.004}$	0.166
$D_{b,\bar{b}}^{\pi^+}(z,m_b^2)$	$N_b^{\pi^+} z^{-1.075}(1-z)^{7.220}$	0.227
$D_{\bar{s}}^{K^+}(z,\mu_0^2)$	$N_{\bar{s}}^{K^+} z^{1.072}(1-z)^{1.316}$	0.148
$D_u^{K^+}(z,\mu_0^2)$	$N_{\bar{s}}^{K^+} z^{1.072}(1-z)^{2.316}$	0.064
$D_{d,\bar{d}}^{K^+}(z,\mu_0^2)$	$N_{\bar{s}}^{K^+} z^{1.072}(1-z)^{3.316}$	0.033
$D_g^{K^+}(z,\mu_0^2)$	$N_g^{K^+} z^{5.610}(1-z)^{5.889}$	0.048
$D_{c,\bar{c}}^{K^+}(z,m_c^2)$	$N_c^{K^+} z^{0.589}(1-z)^{5.162}$	0.074
$D_{b,\bar{b}}^{K^+}(z,m_b^2)$	$N_b^{K^+} z^{-0.086}(1-z)^{7.998}$	0.052
$D_q^{\mathrm{res.}}(z,\mu_0^2)$	$N_q^{\mathrm{res.}}\ z^{1.006}\ (1-z)^{5.843}$	0.043
$D_g^{\mathrm{res.}}(z,\mu_0^2)$	$N_g^{\mathrm{res.}}\ z^{6.387}\ (1-z)^{6.435}$	0.088
$D_c^{\mathrm{res.}}(z,m_c^2)$	$N_c^{\mathrm{res.}}\ z^{-1.103}\ (1-z)^{3.917}$	0.082
$D_b^{\mathrm{res.}}(z,m_b^2)$	$N_b^{\mathrm{res.}}\ z^{-0.605}\ (1-z)^{3.330}$	0.113

Table 1: Numerical values for the NLO fit parameters in Eqs. (22)-(23), (27). The input scales are $\mu_0^2, m_c^2, m_b^2 = 0.4, 1.96, 20.25\mathrm{GeV}^2$ [1]. The Normalizations N_i^h are determined by the second moments of the input functions. These moments evolve rather mildly (typically less than 10% up to M_Z^2) to higher scales due to the constraint (25).

6 Results and Discussion

The quality of the fit can be inferred from Figs. 1, 2, and 3. All non-b event samples can be well described within errors, even the (non-b-tagged) ALEPH data where the error is dominated by a normalization uncertainty of only 1%. As already noted in [17, 53] the b quark fragmentation spectrum can not be described perfectly well using the simple functional form (16) as input to the evolution. The b sets are only reproducible at some 5% accuracy. With the inherent uncertainty due to weak decays we consider this a reasonable precision and do not investigate more involved functional Ansätze for the D_b^h. Note that the longitudinal cross section (lowest curve in Fig. 1), calculated along [29], has not been included in the fit. We list in Table 1 the input functions introduced

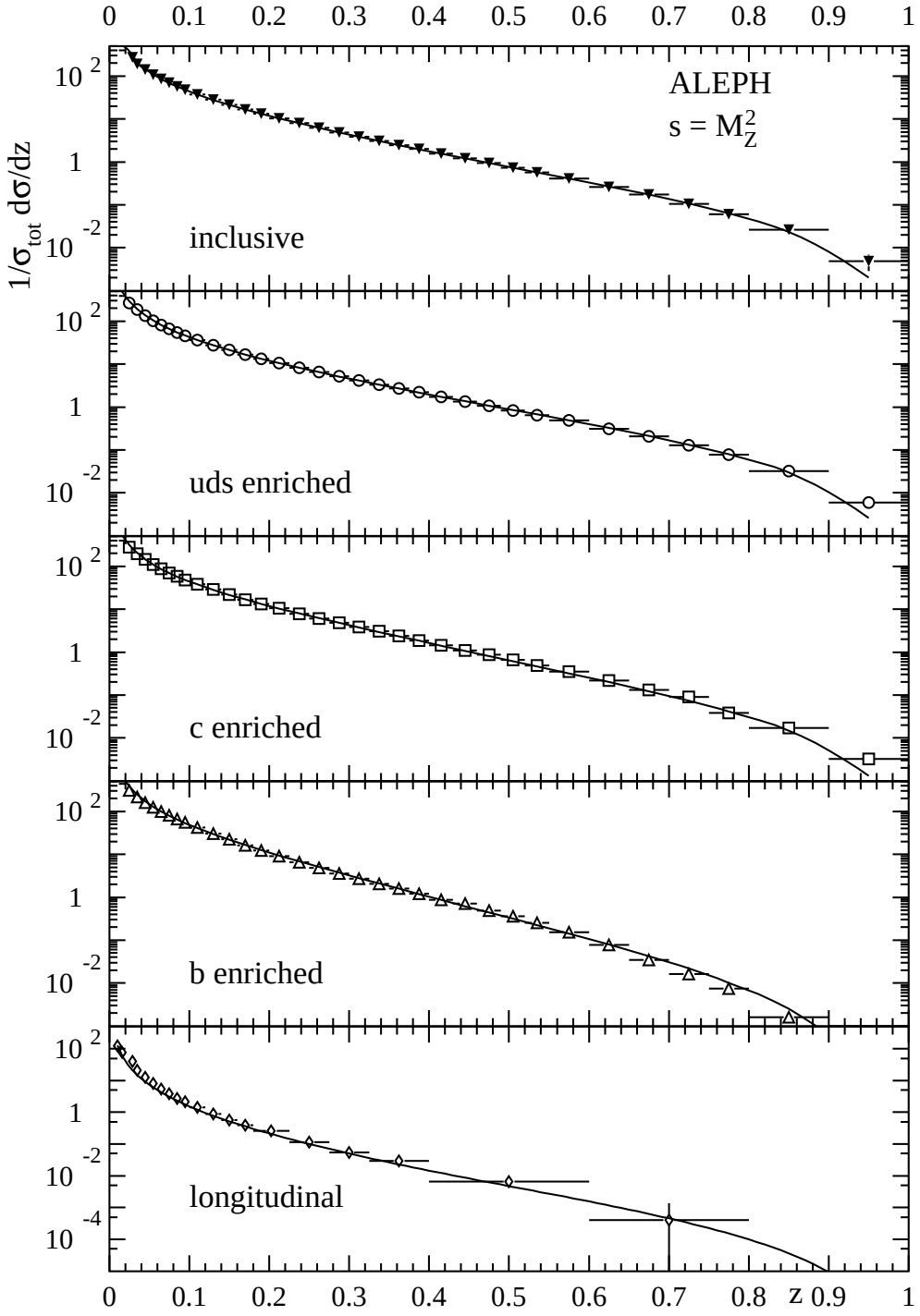

Figure 1: ALEPH [17] $\sum h^{\pm}$ inclusive particle spectra, measured at the Z^0 pole, and the corresponding fit results. Details to the individual data samples and curves are given in the text. The 'longitudinal' set has not been included in the fit.

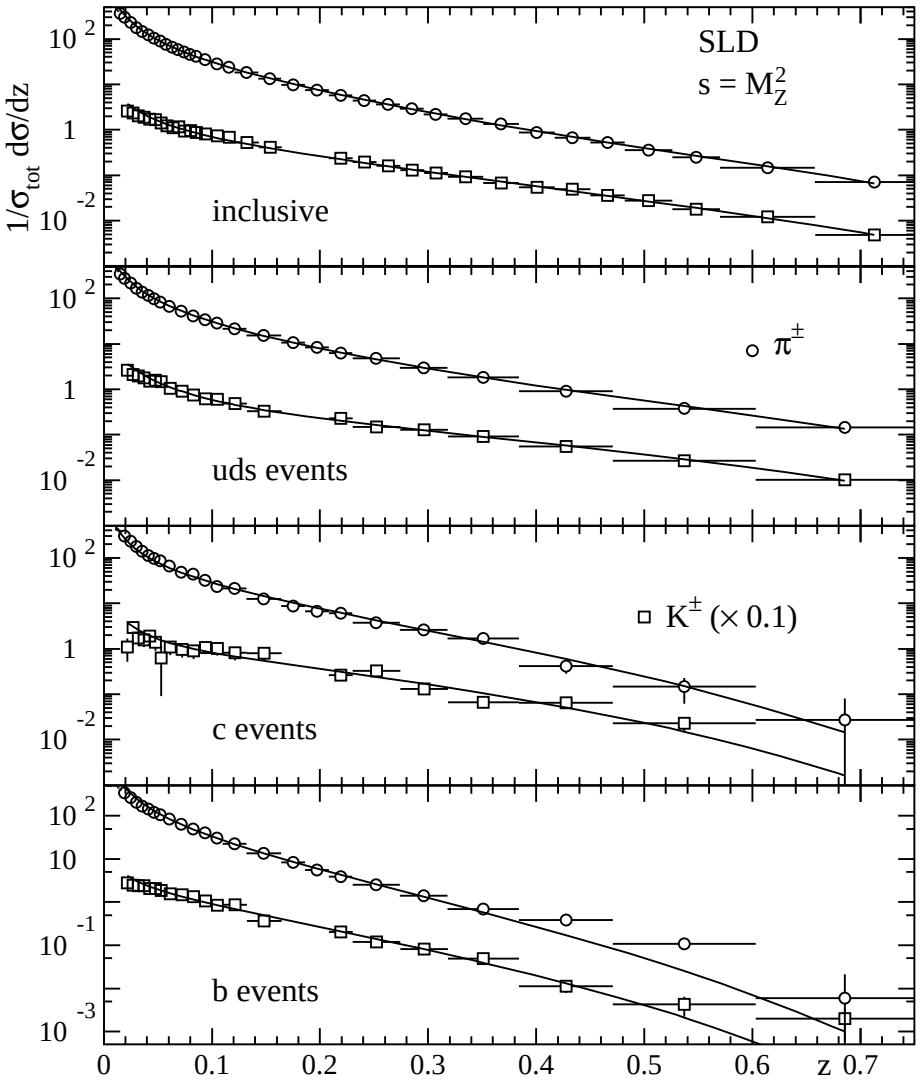

Figure 2: SLD [21] $\pi^\pm$ and $K^\pm$ inclusive particle spectra, measured at the Z^0 pole, and the corresponding fit results. Details to the individual data samples are given in the text.

in Eqs. (22)-(23), (27) along with their contributions to the energy integral (7). As a representative we show the set $D_i^{\pi^+}$ of input fragmentation functions into (positively) charged pions in Fig. 4. Evolution effects to higher scales can be inferred for the low input scale ($\mu_0^2 = 0.4$ GeV^2 [1]) functions $D_{i=u,d,s,g}^{\pi^+}$ from Fig. 5. They are quite dramatic for the gluon FF but less pronounced for the light flavours. For the higher scale ($m_{c,b}^2$) input functions $D_{c,b}^{\pi^+}$, not shown in this Figure, the evolution effects are of course still weaker as for $D_{u,d,s}^{\pi^+}$. The peculiar shape of the input $D_g^{\pi^+}(z, \mu_0^2)$ should be traced back to starting the evolution at the low input scale of [1] thereby maximizing the driving

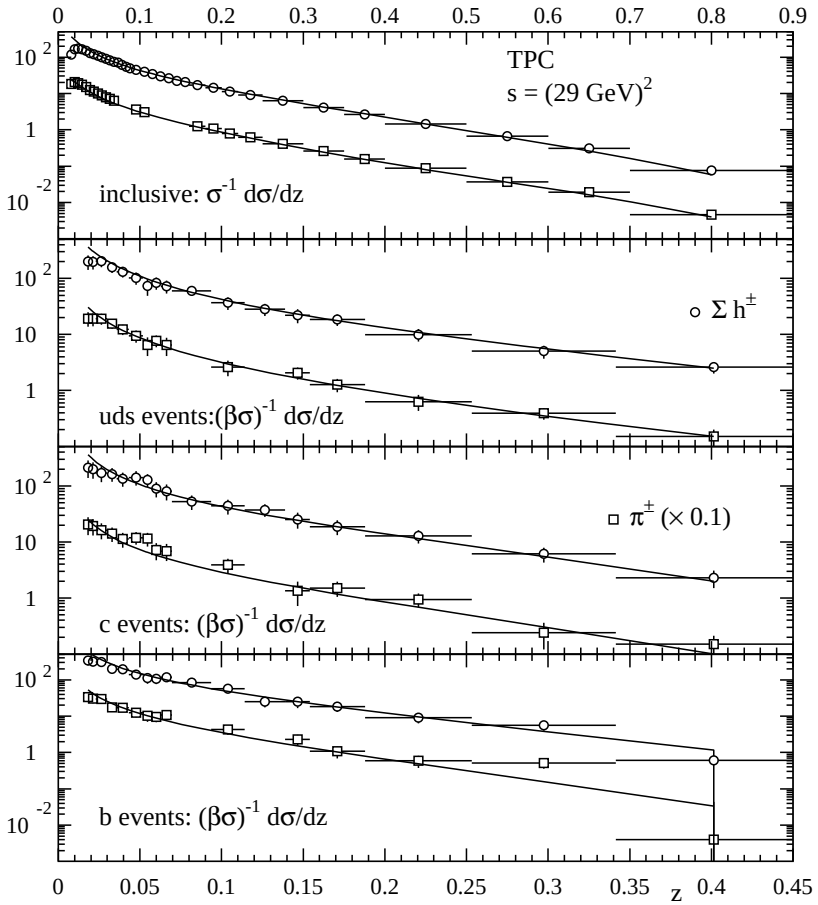

Figure 3: $\sum h^{\pm}$ and $\pi^{\pm}$ inclusive particle spectra and flavour separated events over the range $0 < z < 0.9$ (inclusive) and $0 < z < 0.45$ ($\{u, d, s\}$, c, and b events; $\beta = p_\pi/E_\pi \simeq 1$ for not too small z) as measured at $\sqrt{s} = 29$ GeV by TPC [22]. The corresponding curves are the fit results. Details to the individual data samples and curves are given in the text. Also included in the fit were inclusive $K^{\pm}$ data by TPC which are, however, not accompanied by flavour tagged samples and are therefore not shown in the Figure for clearness.

force of $D_g^{\pi^+}$. From pion dominance we would assume a value of $D_i^{\Sigma h^{\pm}}(n = 2) \lesssim 2/3$ and it is interesting that this expectation is roughly confirmed. Also, estimating the contributions from neutral hadrons from $\mathrm{SU(2)_f}$ symmetry results in values for the r.h.s. of Eq. (7) within $[0.9; 1.0]$ which confirms energy conservation (8) except for $D_b^{\Sigma h}$ which violates (8) to about $\sim 10\%$. However, as mentioned above, a pure QCD fit to bottom fragmentation is questionable due to weak decay channels which mostly contaminate b jets. Furthermore, a physical interpretation of the second moment integrals (24) over the range $z\epsilon[0; 1]$ is delicate and may be misleading in general due to a sizable contribution

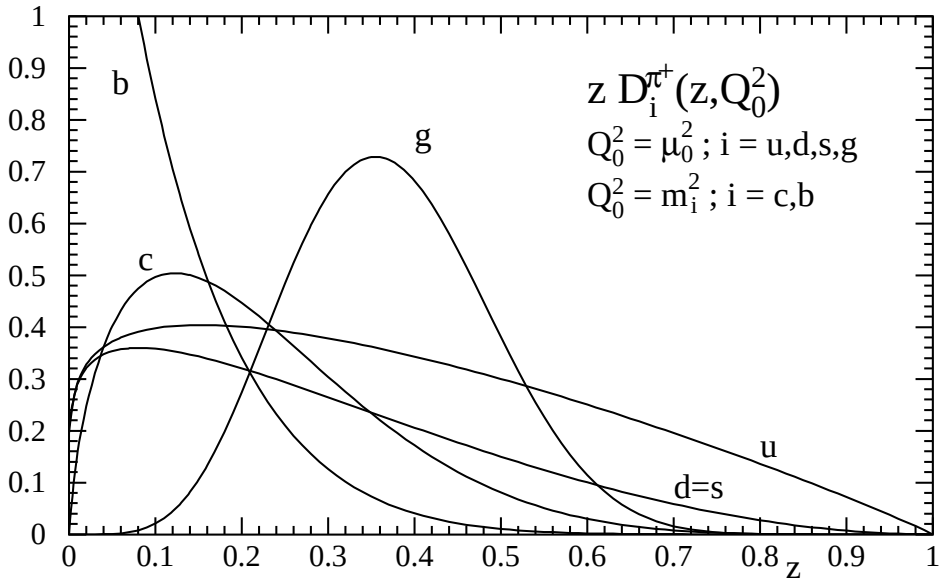

Figure 4: The input fragmentation functions $D_i^{\pi^+}$ as given in Table 1 at their respective input scales.

from the perturbatively unstable very low z region, as we will discuss in more detail in Section 6.2.

We have also evolved our $\sum h^{\pm}$ fit to a c.m.s. energy of $\sqrt{s} = 161$ GeV and compared the evolution to measurements by OPAL [54] in Fig. 6. The agreement is convincing albeit not too surprising because scaling violations from $M_Z \to 161$ GeV are rather moderate. In Figs. 7 and 8 we compare our fitted fragmentation functions to a previous NLO fit by Binnewies, Kniehl and Kramer (BKK) [5]. These authors confirm QCD scaling violations within a wider range of data, albeit not with the flavour information of Ref. [21] on the individual $\pi^{\pm}$ and $K^{\pm}$ spectra. Instead, the flavour separation in [5] was done by fitting to the flavour tagged ALEPH [17] $\sum h^{\pm}$ data and assuming $d\sigma^{\Sigma h^{\pm}} = d\sigma^{(\pi+K)^{\pm}} + f$ where f is a small residual from (anti-)protons as measured in [55]. Besides discrepancies in the barely constrained D_g^h, our procedure of decoupled fits to $\sum h^{\pm}$, $\pi^{\pm}$ and $K^{\pm}$ data yields quite different results for the individual flavour fragmentation functions into $\pi^{\pm}$ and $K^{\pm}$. Note that the differences of our fit to BKK decrease stepwise the more flavour-inclusive sums of FFs are considered. For the 'democratic' FF $D_{u+d+s+c+b}^{(\pi+K)^{\pm}}$ the difference shrinks to at most 4% within $0.1 < z < 0.8$. In any case, the light flavour (uds) structure is, at

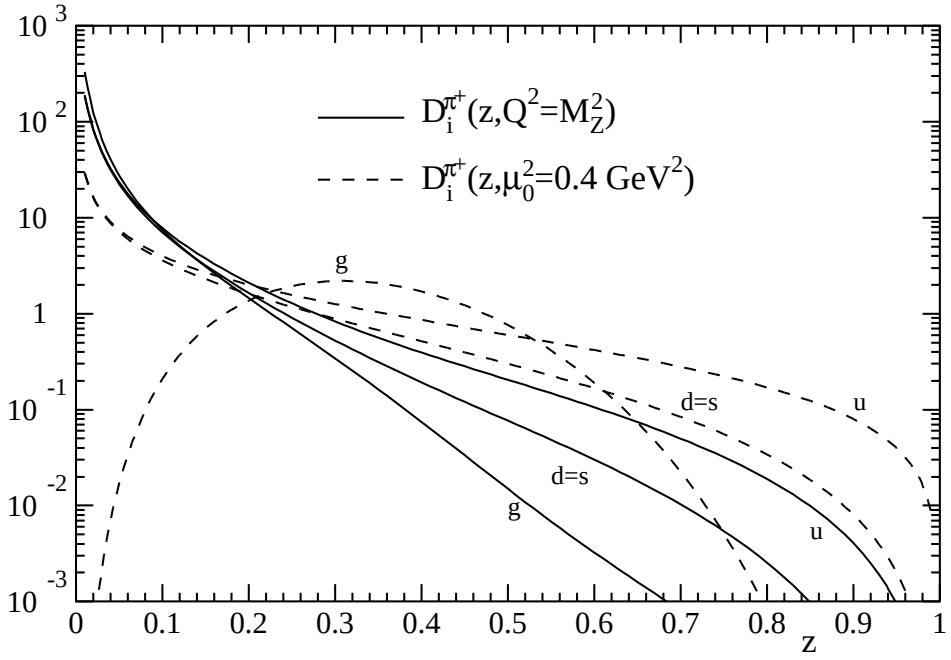

Figure 5: The input for light (uds) quarks and gluons of Fig. 4 evolved upward to $Q^2 = M_Z^2$.

present, arbitrary to some extent in our fit as well as the one of Ref. [5] and differences between the two fits of the individual $D_{i=u,d,s}^{\Sigma h^\pm}$ estimate the present uncertainty on these functions.

6.1 3-Jet Measurements and Gluon Fragmentation; Leading Particle Effects

Complementary to our considerations of one-particle inclusive e^+e^- annihilation data, individual quark and gluon fragmentation functions can also be derived from 3-jet topologies [56–58] which can at the leading perturbative order be attributed to partonic $q\bar{q}g$ configurations and where an experimental fragmentation function can be defined as

$$D_i^h(x_E,\mu^2) \equiv \frac{1}{N_{\mathrm{tot}}}\,\frac{\Delta N_i^h}{\Delta x_E}; \quad x_E \equiv \frac{E_h}{E_i^{\mathrm{jet}}}; \tag{28}$$

i.e. as the spectrum in energy E_h scaled to the jet energy E_i^{jet} of some hadron species h distributed inside a jet initiated by a parton i. In general, QCD scale dependence from

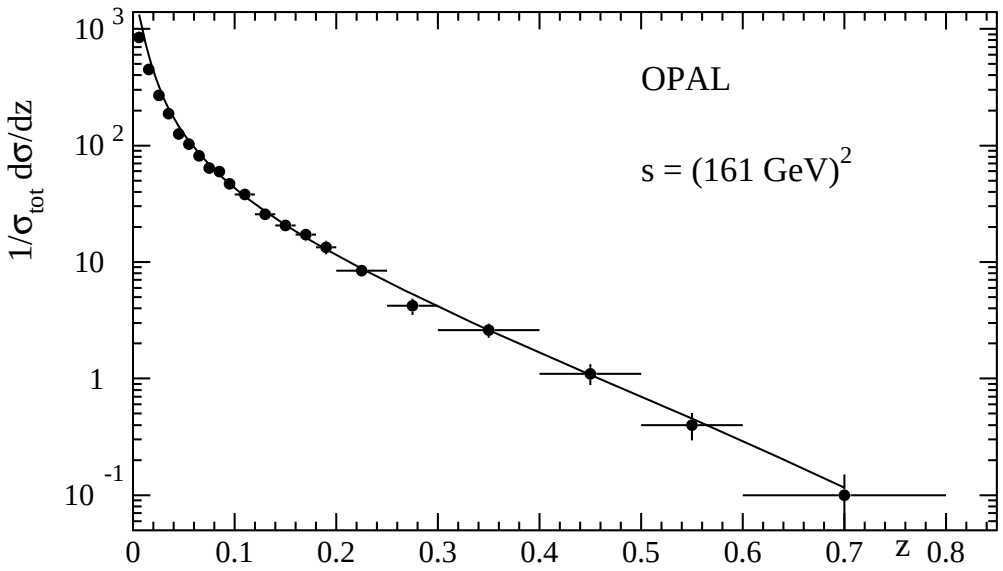

Figure 6: OPAL inclusive $\sum h^{\pm}$ particle spectrum measured at a c.m.s. energy of $\sqrt{s} =$ 161 GeV. The curve is the fit of Fig. 1 evolved upward to that energy.

leading logarithms can be understood non-covariantly from the transverse phase space volume available for collinear parton emission (*splitting* process)

$$\int_{\mu^2}^{(p_\perp^{\max})^2} \frac{dp_\perp^2}{p_\perp^2} \left[P_{ji}^{(0)}(z)\right]_{p_\perp=0} = P_{ji}^{(0)}(z) \ln\left(\frac{p_\perp^{\max}}{\mu}\right)^2 \tag{29}$$

and a phase space boundary $(p_\perp^{\max})^2 = \mathcal{O}(s)$ leads to the common choice $\mu = \sqrt{s} = Q$ for an (one-particle-)inclusive phase space. A different $p_\perp^{\max}$ is, however, induced in a three jet topology from the requirement that parton emission proceeds into a cone the geometry of which is defined by the hadrons which are grouped together as the jet. The analysis in [58] has demonstrated the fragmentation function defined in Eq. (28) to undergo scaling violations compatible with LO QCD evolution in the jet topology scale $\mu = E^{\rm jet} \sin(\theta/2)$ where θ is the angle to the nearest jet in a 3-jet event. For the time being, these considerations have to be restricted to a LO treatment, since NLO corrections (stemming e.g. from a kinematical configuration where the quark of the $q\bar{q}g$ triple emits a high $p_\perp$ gluon into the jet clustered around the anti-quark) have to our knowledge not been formulated yet and we have therefore refrained from including the data of [56–58] in our fits. The gluon fragmentation function D_g^h is, however, barely constrained from

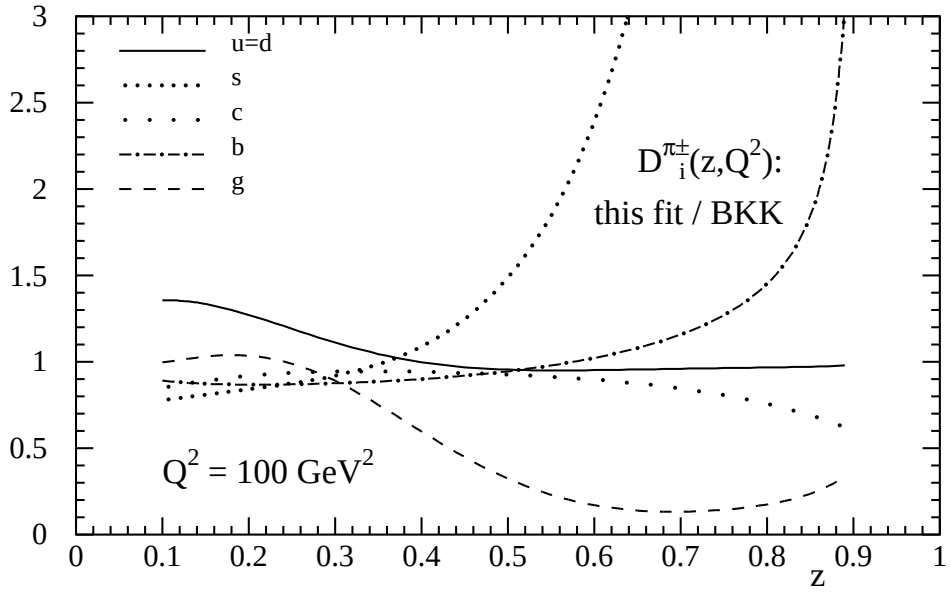

Figure 7: Ratios of the individual fragmentation functions obtained from this NLO fit to their analogues in Ref. [5].

one-particle-inclusive final state measurements in e^+e^- annihilation because it enters the cross section in Eqs. (5), (6) only in subleading order $\mathcal{O}(\alpha_s^1)$ and where the leading part is factorized into the evolution (9) where D_g^h mixes with the quark singlet fragmentation function $\sum_q D_q^h$. Therefore, keeping the vagueness of this comparison in mind we use the 3-jet data of Ref. [57] to compare our fitted $D_g^{\Sigma h^\pm}(z,\mu^2)$ with, i.e. we compare $D_g^{\Sigma h^\pm}\left(z=x_E,\mu^2=\left\langle E_g^{\rm jet}\right\rangle^2\simeq(40{\rm GeV})^2\right)$ with the measured $\frac{1}{N_{\rm tot}}\,\frac{\Delta N}{\Delta x_E}$ in Eq. (28) for the time being, with the *caveat* that this cannot give us more than an idea of the compatibility of our NLO gluon FF with 3-jet measurements. For illustration we also include the gluon fragmentation function of [5] [using the approximation (26)] and an independent experimental LO determination from DELPHI [58] in our comparison. Hence, the discrepancy between the data [57] and the LO QCD fit to an independent measurement [58] estimates the accuracy to which the 3-jet data [57] can be identified with a QCD gluonic fragmentation function. From Fig. 9 we judge that the result seems promising and that a refinement of the theoretical framework would probably contribute to removing the existing ambiguities in the gluon fragmentation function.

Similar theoretical limitations as outlined above for 3-jet measurements also prevent

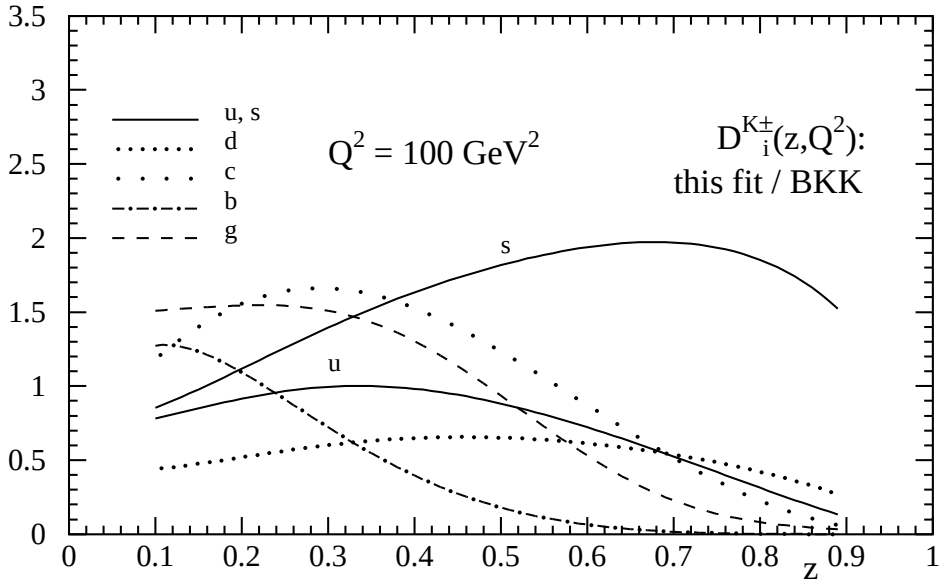

Figure 8: Same as Fig. 7 but for the fragmentation functions into charged Kaons $K^{\pm}$.

at present a detailed pQCD analysis of leading particle effects [50] in e^+e^- annihilations which are based experimentally on phase space restrictions which do not fully match a one-particle inclusive QCD framework. Qualitatively, the results of the leading particle measurements in [50] are accounted for by Eq. (20).

6.2 Perturbative Stability and Energy Sum Rule

The full NLO framework of Section 2 is expected to yield more reliable and less scale-sensitive results compared to a LO truncation of the perturbation series where the known $\mathcal{O}(\alpha_s)$ terms of the coefficient functions (6) are neglected as well as the β_1 contribution to the running of α_s and where the omission of the $P_{ij}^{(1)}$ parts of the splitting functions reduces the evolution (9) to summing only the most dominantly leading logs $(\alpha_s/2\pi \ln Q^2)^n$ for all n. Still, an accompanying LO fit is - besides future effective LO applications - valuable as a test of the perturbative LO↔NLO stability which is a delicate requirement for perturbative (QCD) approaches to strong interaction phenomena - especially if the perturbative QCD dynamics is supposed to set in at the rather low input scale in (11) taken from [1]. For infrared *un*safe quantities - such as the one-particle-inclusive spectra

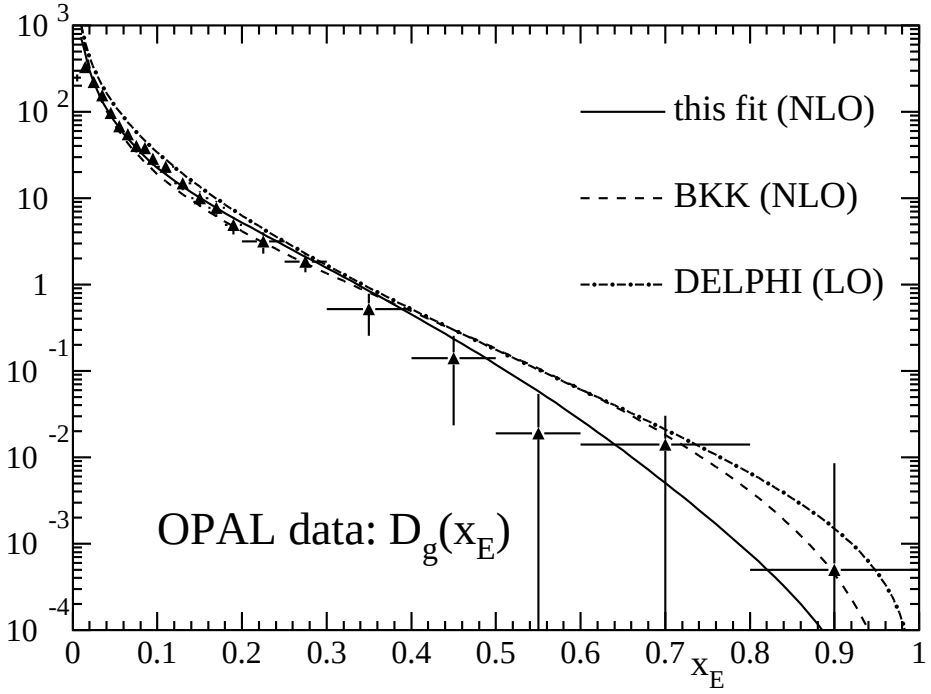

Figure 9: The gluon fragmentation function as defined experimentally in (28) and measured by OPAL [57] compared to the NLO fits of our analysis as well as the one in [5]. An experimental LO determination from DELPHI [58] is also included for comparison.

considered here - the nonperturbative parameters have to be redefined at each perturbative order since they replace new infrared sensitive terms of the factorized perturbation series at any order. We have accordingly performed an accompanying LO fit following exactly the same lines as the NLO fit described above and resulting in Table 2. In order not to overload the logarithmic-scale figures of the preceding sections with narrow pairs (LO, NLO) of lines and instead of repeating the details for the LO fitting procedure we rather concentrate in this separate Section on two LO↔NLO issues worth mentioning. As a representative we will consider our sets of pionic fragmentation functions. In Fig. 10 we show K-factors for $d\sigma$ in Eq. (1), $K \equiv d\sigma^h_{\rm NLO}/d\sigma^h_{\rm LO}$, as well as for each flavour contribution

$$\mathcal{D}_q^{\pi^\pm}(z,Q^2) \equiv \left[\left(D_q^{\pi^\pm} + D_{\bar{q}}^{\pi^\pm}\right) \otimes C_{T+L}^q\right](z,Q^2) + \left[D_g^{\pi^\pm} \otimes \overline{C}_{T+L}^g\right](z,Q^2) \qquad (30)$$

where $\overline{C}_{T+L}^g \equiv C_{T+L}^g \times [\sigma_0^q / \sum_{q'} \sigma_0^{q'}]$ is the C_{T+L}^g of Eq. (6) 'per flavour' and where $\otimes$ denotes a convolution integral as in Eq. (5). Note that the $\mathcal{O}(\alpha_s^1)$ terms of Eq. (6) entering Eq. (30) in NLO are neglected in LO where only the $\sim \delta(1-z)$ term of C_T^q contributes. The vertical lines in Fig. 10 indicate the range in z where the fit is rather

$D_i^h(z,Q_0^2)$	$N_i^h\ z^{\alpha_i^h}\ (1-z)^{\beta_i^h}$	$D_i^h(n=2,Q_0^2)$
$D_{u,\bar{d}}^{\pi^+}(z,\mu_0^2)$	$N_u^{\pi^+} z^{-0.923}(1-z)^{0.976}$	0.377
$D_{s,\bar{s}}^{\pi^+}(z,\mu_0^2)$	$N_u^{\pi^+} z^{-0.923}(1-z)^{1.976}$	0.244
$D_g^{\pi^+}(z,\mu_0^2)$	$N_g^{\pi^+} z^{5.271}(1-z)^{8.235}$	0.311
$D_{c,\bar{c}}^{\pi^+}(z,m_c^2)$	$N_c^{\pi^+} z^{-0.818}(1-z)^{3.461}$	0.241
$D_{b,\bar{b}}^{\pi^+}(z,m_b^2)$	$N_b^{\pi^+} z^{-1.072}(1-z)^{6.695}$	0.264
$D_{\bar{s}}^{K^+}(z,\mu_0^2)$	$N_{\bar{s}}^{K^+} z^{0.617}(1-z)^{0.744}$	0.213
$D_u^{K^+}(z,\mu_0^2)$	$N_{\bar{s}}^{K^+} z^{0.617}(1-z)^{1.744}$	0.085
$D_{d,\bar{d}}^{K^+}(z,\mu_0^2)$	$N_{\bar{s}}^{K^+} z^{0.617}(1-z)^{2.744}$	0.044
$D_g^{K^+}(z,\mu_0^2)$	$N_g^{K^+} z^{8.132}(1-z)^{5.776}$	0.064
$D_{c,\bar{c}}^{K^+}(z,m_c^2)$	$N_c^{K^+} z^{1.419}(1-z)^{6.171}$	0.085
$D_{b,\bar{b}}^{K^+}(z,m_b^2)$	$N_b^{K^+} z^{0.191}(1-z)^{8.934}$	0.062
$D_q^{\text{res.}}(z,\mu_0^2)$	$N_q^{\text{res.}}\ z^{0.938}\ (1-z)^{7.734}$	0.146
$D_g^{\text{res.}}(z,\mu_0^2)$	$N_g^{\text{res.}}\ z^{6.150}\ (1-z)^{5.379}$	0.003
$D_c^{\text{res.}}(z,m_c^2)$	$N_c^{\text{res.}}\ z^{-0.636}\ (1-z)^{2.486}$	0.084
$D_b^{\text{res.}}(z,m_b^2)$	$N_b^{\text{res.}}\ z^{-0.736}\ (1-z)^{3.012}$	0.137

Table 2: Input parameters as in Table 1 but for our LO fit where $\mu_0^2 = 0.26\text{GeV}^2$ [1].

well determined, where $z > 0.05$ excludes the perturbatively unstable [16] low z region and where for $z \gtrsim 0.7$ statistics drop rather low (only one data point for $z > 0.7$). Hence, the spread of the curves towards large z should not be taken as a perturbative instablitiy but attributed mainly to the decreasing experimental statistics which do not determine the FFs very well [18] in the $z \to 1$ hard fragmentation limit and where poorly defined χ^2 minima may easily fake perturbative instability in decoupled LO$\leftrightarrow$NLO fits. It is therefore reassuring to observe that the flavour-inclusive $d\sigma$ has a K-factor closer to one than the individual flavour-contributions where the latter have poorer experimental statistics and larger systematic errors than the former. On the other hand, the unstable $z \to 0$ behaviour is unaffected by the choice of input parameters and can be traced back to including/omitting the NLO pieces $P_{ij}^{(1)}$ of the splitting functions in the NLO/LO evolution. Indeed, our choice $z_{\min} = 0.05$ appears already to be on the edge of perturbative reliability. The far steeper LO evolution has profound impact on the second moments in Table 2 which violate the energy sum rule (8). We demonstrate this point in Fig. 11

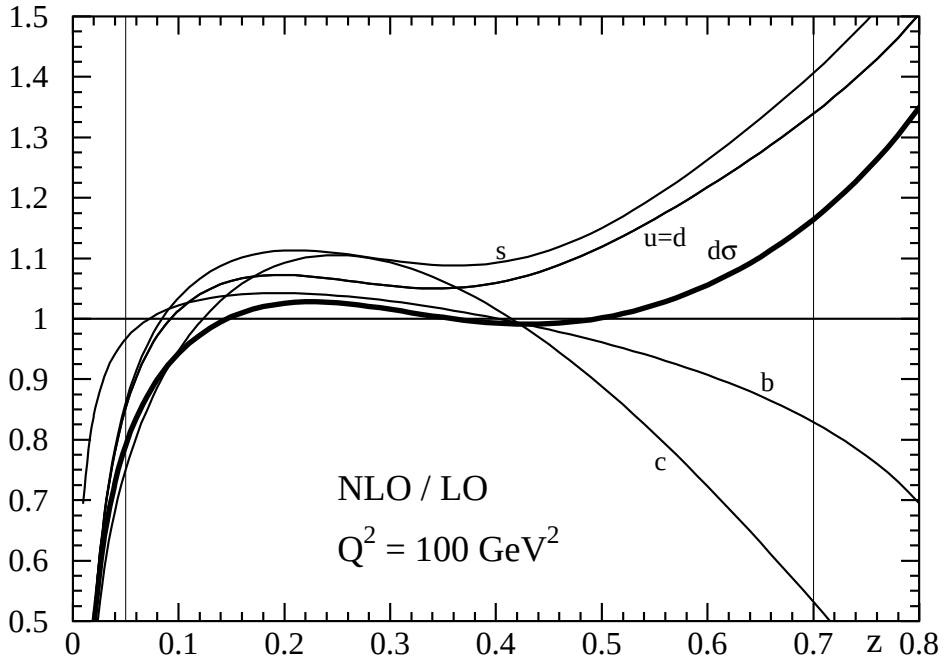

Figure 10: K-factors for individual flavours and inclusive charged pion production. The vertical lines indicate the range where the fit is rather well defined where $z_{\min}$ is set by perturbative stability and $z_{\max}$ by experimental statistics.

where we show the truncated moment

$$\frac{\int_{z_{\min}}^{1} dz\ z\ \mathcal{D}_u^{\pi^+}(z,Q^2)}{\mathcal{D}_u^{\pi^+}(n=2,Q^2)} \tag{31}$$

in LO and NLO. It can be seen that the full second moment receives in LO a sizable contribution from the unstable $z < 0.05$ region where the evolution generates a too steep spectrum resulting in large second moments violating (8). On the other hand, in NLO the second moment, truncated at $z_{\min} = 0.05$, is rather close to its *un*truncated value leading to NLO moments that compare rather well with (8). One must note, however, that the choice $z_{\min} = 0.05$ is rather arbitrary and that the region $z\epsilon[0.0; 0.05]$ does not contribute much in NLO partly because $\mathcal{D}_q^{\pi^\pm}(z,Q^2)$ turns *un*physically *negative* at very small z due to the timelike NLO evolution [16]. This observation renders the energy sum rule (8) a delicate concept for perturbative QCD FFs and we believe it should not be considered within this theoretical framework unless the $z \to 0$ behaviour of FFs is under better control.

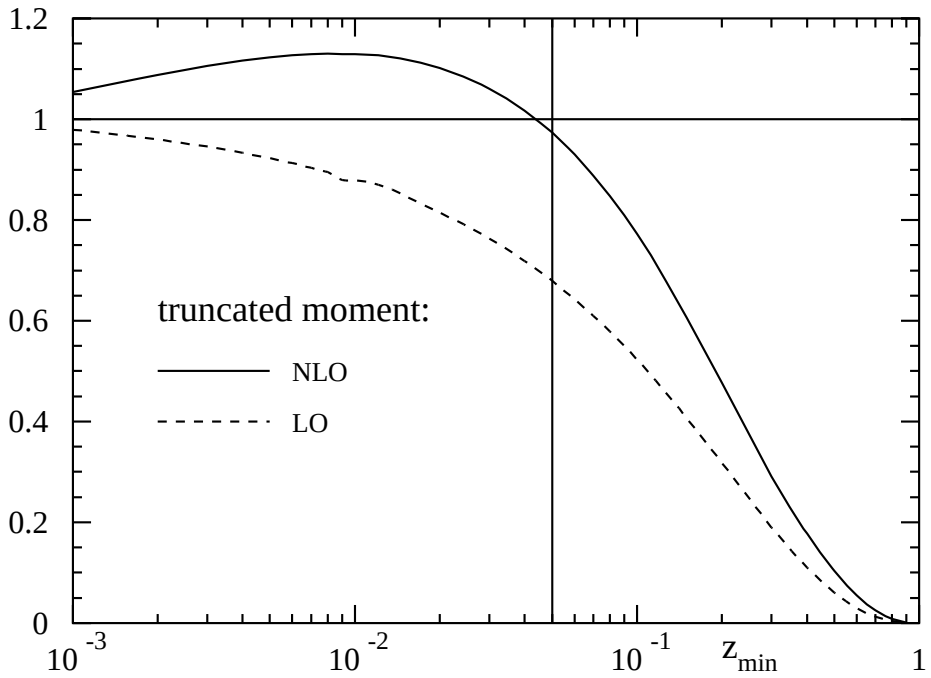

Figure 11: The truncated second moment of the u-quark contribution to charged pion production as defined in Eqs. (30), (31). Shown are results for our NLO and LO fit.

7 Conclusions

Within the radiative parton model [1, 30–33] we have fitted parton fragmentation functions to identified hadron ($\pi^{\pm}$, $K^{\pm}$) and inclusive charged particle spectra measured at the Z^0 pole [17, 21]. Scaling violations were properly taken into account by simultaneously fitting lower energy TPC data. Special attention was paid to the flavour structure of the parton FFs where a collinearly resummed RGE formalism was argued to be adequate for the treatment of heavy quark contributions. In the light quark sector we made power law assumptions which qualitatively establish a physical hierarchy among the FFs which is guided by the ideas of valence enhancement and strangeness suppression and which is observed in leading particle measurements. It would be desirable to interpret these measurements - as well as gluon-jet measurements from 3-jet topologies - in more quantitative detail within the language of NLO QCD fragmentation functions. A corresponding framework has, however, to our knowledge not been developed yet. Despite the high precision data available, the *individual* $D_{i=u,d,s,g,c,b}^{\Sigma h^{\pm},\pi^{\pm},K^{\pm}}$ are therefore still rather uncertain. To estimate

the present theoretical uncertainty we compared our fit to the one of [5] and found sizable deviations. An inclusive sum over the distinct flavours is, however, rather reliably determined for not too large z. The missing experimental information at large z may fake perturbative instability in independent LO↔NLO fits manifesting, however, just the fact that the FFs are still unknown in the $z \to 1$ hard fragmentation limit. We also considered the contributions of the individual FFs to the energy integral in (7) and found reasonable values in NLO while the steeper LO evolution requires too large moments. The instability of the timelike evolution at low z makes, however, energy conservation a concept which may hardly be useful within perturbative QCD even for NLO FFs.

A `FORTRAN` package of the LO and NLO D_i^h-functions will be obtainable upon request.

Acknowledgements

We thank E. Reya and M. Glück for suggestions and many instructive discussions, I. Schienbein for helpful discussions and a careful reading, and W. Bernreuther, A. Brandenburg and P. Uwer for helpful correspondences. We are thankful to W. Hofmann for making Tables of the flavour tagged TPC data accessible to us. The work has been supported in part by the 'Bundesministerium für Bildung, Wissenschaft, Forschung und Technologie', Bonn.

Appendix: $\overline{\rm MS}$ Coefficient Functions for One Hadron Inclusive e^+e^- Annihilation

The $\mathcal{O}(\alpha_s^1)$ coefficient functions for One Hadron Inclusive e^+e^- Annihilation as introduced in Section 1 read [11, 23, 24]:

$$\begin{aligned}
c_T^q\left(\zeta,\frac{Q^2}{\mu_F^2}\right) &= (1+\zeta^2)\left[\frac{\ln(1-\zeta)}{1-\zeta}\right]_+ - \frac{3}{2}\left[\frac{1}{1-\zeta}\right]_+ + 2\frac{1+\zeta^2}{1-\zeta}\ln\zeta \\
&+ \frac{3}{2}(1-\zeta) + (\frac{2}{3}\pi^2 - \frac{9}{2})\delta(1-\zeta) + \ln\frac{Q^2}{\mu_F^2}\left[\frac{1+\zeta^2}{1-\zeta}\right]_+ \quad , \\
c_T^g\left(\zeta,\frac{Q^2}{\mu_F^2}\right) &= 2\frac{1+(1-\zeta)^2}{\zeta}\left(\ln(1-\zeta) + 2\ln\zeta + \ln\frac{Q^2}{\mu_F^2}\right) - 4\frac{1-\zeta}{\zeta} \quad , \\
c_L^q\left(\zeta,\frac{Q^2}{\mu_F^2}\right) &= 1 \quad , \\
c_L^g\left(\zeta,\frac{Q^2}{\mu_F^2}\right) &= 4\frac{1-\zeta}{\zeta} \quad . \qquad (32)
\end{aligned}$$

The parton model, i.e. $\mathcal{O}(\alpha_s^0)$ electroweak cross section σ_0^q for producing a $q\bar{q}$ pair in e^+e^- annihilation are given by

$$\sigma_0^q(s) = \frac{4\pi\alpha^2}{s}\ \left[e_q^2 + 2e_q v_e v_f \rho_1(s) + (v_e^2+a_e^2)(v_q^2+a_q^2)\rho_2(s)\right] \qquad (33)$$

with the QED fine structure constant α and where

$$\begin{aligned}
\rho_1(s) &= \frac{1}{4\sin^2\theta_W\cos^2\theta_W}\frac{s(M_Z^2-s)}{(M_Z^2-s)^2+M_Z^2\Gamma_Z^2} \quad , \\
\rho_2(s) &= \left(\frac{1}{4\sin^2\theta_W\cos^2\theta_W}\right)^2\frac{s^2}{(M_Z^2-s)^2+M_Z^2\Gamma_Z^2} \quad , \qquad (34)
\end{aligned}$$

and the electric charges e_i and electroweak vector (v_i) and axial (a_i) couplings are listed in Table 3 according to their standard model values:

$$\begin{aligned}
v_i &= T_{3,i} - 2e_i\sin^2\theta_W \\
a_i &= T_{3,i} \quad , \qquad (35)
\end{aligned}$$

where $\vec{T}$ is the weak isospin and θ_W the Weinberg angle.

particle i	e_i	v_i	a_i
e^-	-1	$-\frac{1}{2}+2\sin^2\theta_W$	$-\frac{1}{2}$
up-type quark	$+\frac{2}{3}$	$+\frac{1}{2}-\frac{4}{3}\sin^2\theta_W$	$+\frac{1}{2}$
down-type quark	$-\frac{1}{3}$	$-\frac{1}{2}+\frac{2}{3}\sin^2\theta_W$	$-\frac{1}{2}$

Table 3: Electromagnetic and electroweak couplings entering Eq. (33)

The Mellin transforms of the $c_{T,L}^{q,g}$ in Eq. (32) read [26]

$$\begin{aligned}
c_T^q\left(n,\frac{Q^2}{\mu_F^2}\right) &= 5\mathrm{S}_2(n)+\mathrm{S}_1^2(n)+\mathrm{S}_1(n)\left[\frac{3}{2}-\frac{1}{n(n+1)}\right]-\frac{2}{n^2}+\frac{3}{(n+1)^2} \\
&- \frac{3}{2}\frac{1}{n+1}-\frac{9}{2}+\left[\frac{1}{n(n+1)}-2\mathrm{S}_1(n)+\frac{3}{2}\right]\ln\frac{Q^2}{\mu_F^2} \\
c_T^g\left(n,\frac{Q^2}{\mu_F^2}\right) &= 2\left[-\mathrm{S}_1(n)\frac{n^2+n+2}{(n-1)n(n+1)}-\frac{4}{(n-1)^2}+\frac{4}{n^2}-\frac{3}{(n+1)^2}\right] \\
&+ 2\frac{n^2+n+2}{n(n^2-1)}\ln\frac{Q^2}{\mu_F^2} \\
c_L^q\left(n,\frac{Q^2}{\mu_F^2}\right) &= \frac{1}{n} \\
c_L^g\left(\zeta,\frac{Q^2}{\mu_F^2}\right) &= \frac{4}{(n-1)n} \quad , \qquad (36)
\end{aligned}$$

where the sums

$$\mathrm{S}_k(n)\equiv\sum_{j=1}^{n}\frac{1}{j^k} \qquad (37)$$

have to be analytically continued [31, 36] to the complex n plane

$$\begin{aligned}
\mathrm{S}_1(n) &= \gamma_E+\psi(n+1),\ \gamma_E=0.577216 \\
\mathrm{S}_2(n) &= \zeta(2)-\psi'(n+1),\quad \zeta(2)=\frac{\pi^2}{6} \qquad (38)
\end{aligned}$$

with the help of logarithmic derivatives of the Γ function $\psi^{(k)}(n)\equiv d^{(k+1)}\ln\Gamma(n)/dn^{k+1}$. Analogously to the $\mathcal{O}(\alpha_s^1)$ contribution F_L to the deep inelastic electron nucleon cross section, the $\mathcal{O}(\alpha_s^1)$ contribution from longitudinally polarized virtual bosons to the fragmentation spectrum in e^+e^- annihilations is scheme independent and finite. The $c_L^{q,g}$ do therefore *not* depend on the factorization scale μ_F^2, contrary to the $c_T^{q,g}$ which are infrared safe only after factorization of the collinear singularities.

References

[1] M. Glück, E. Reya and A. Vogt, Eur. Phys. J. **C5**, 461 (1998).

[2] R.D. Field and R.P. Feynman, Nucl. Phys. **B136**, 1 (1978).

[3] J. C. Collins, D. Soper and G. Sterman, in A. H. Mueller, ed., *Perturbative Quantum Chromodynamics* (World Scientific 1989).

[4] J.C. Collins and D.E. Soper, Nucl. Phys. **B193**, 381 (1981), **B213**, 545 (1983) (E); **B194** 445 (1982).

[5] J. Binnewies, B.A. Kniehl, G. Kramer, Phys. Rev. **D52**, 4947 (1995).

[6] K. Ackerstaff *et al.*, HERMES Collab., Phys. Rev. Lett. **81**, 5519 (1998); Phys. Lett. **B464**, 123-134 (1999); B. Adeva *et al.*, SM Collab., Phys. Lett. **B369**, 93 (1997); Phys. Lett. **B420**, 180 (1998).

[7] M. Arneodo *et al.*, EM Collab., Nucl. Phys. **B321**, 541 (1989).

[8] P. Geiger, Ph.D. Thesis, Ruprecht-Karls-Universität Heidelberg, February 1998.

[9] L.L. Frankfurt, M.I. Strikman, L. Mankiewicz, A. Schäfer, E. Rondio, A. Sandacz and V. Papavassiliou, Phys. Lett. **B230**, 141 (1989); D. de Florian O.A. Sampayo and R. Sassot, Phys. Rev. **D57**, 5803 (1998); E. Christova and E. Leader, Phys. Lett. **B468**, 299 (1999); T. Morii and T. Yamanishi, Phys. Rev. **D61**, 057501 (2000).

[10] Research to be pursued by the author.

[11] P. Nason and B. R. Webber, Nucl. Phys. **B421**, 473 (1994); **480**, 755 (1996) (E).

[12] P. Chiappetta, M. Greco, J.Ph. Guillet, S. Rolli and M. Werlen, Nucl. Phys. **B412**, 3 (1994); M. Greco, S. Rolli and A. Vicini, Z. Phys. **C65**, 277 (1995); M. Greco and S. Rolli, Phys. Rev. **D52**, 3853 (1995); M. Greco and S. Rolli, Z. Phys. **C60**, 169 (1993).

[13] J. Binnewies, B.A. Kniehl, G. Kramer, Z. Phys. **C65**, 471 (1995).

[14] J. Binnewies, B.A. Kniehl, G. Kramer, Phys. Rev. **D53**, 3573 (1996); Phys. Rev. **D53**, 6110 (1996).

[15] D. Indumathi, H.S. Mani and Anubha Rastogi, Phys. Rev. **D58**, 094014 (1998).

[16] D. de Florian, M. Stratmann, W. Vogelsang, Phys. Rev. **D57**, 5811 (1998).

[17] D. Buskulic *et al.*, ALEPH Collab., Phys. Lett. **B357**, 487 (1995); Phys. Lett. **B364**, 247 (1995) (E); C.P. Padilla Aranda, Ph.D. Thesis, Universitat Autònoma de Barcelona, September 1995.

[18] P. Aurenche, M. Fontanaz, J.-Ph. Guillet, B.A. Kniehl, and M. Werlen, `hep-ph/9910252`.

[19] A.D. Martin, R.G. Roberts, W.J. Stirling, and R.S. Thorne, Eur. Phys. J. **C4**, 463 (1998).

[20] H. L. Lai *et al.*, CTEQ Collab., `hep-ph/9903282`.

[21] K. Abe *et al.*, SLD Collab., Phys. Rev. **D59**, 052001 (1999).

[22] H. Aihara *et al.*, TP Collab., Phys. Rev. Lett. **61**, 1263 (1988); Xing-Qi Lu, Ph.D. Thesis, John Hopkins University, 1986.

[23] G. Altarelli, R. K. Ellis, G. Martinelli and S.–Y. Pi, Nucl. Phys. **B160**, 301 (1979).

[24] W. Furmanski and R. Petronzio, Z. Phys. **C11**, 293 (1982).

[25] G. Curci, W. Furmanski and R. Petronzio, Nucl. Phys. **B175**, 27 (1980); W. Furmanski and R. Petronzio, Phys. Lett. **97B**, 437 (1980); P.J. Rijken and W.L. van Neerven, Nucl. Phys. **B487**, 233 (1997).

[26] M. Glück, E. Reya and A. Vogt, Phys. Rev. **D48**, 116 (1993); **D51**, 1427 (1995) (E).

[27] M. Stratmann and W. Vogelsang, Nucl. Phys. **B496**, 41 (1997).

[28] M. Dasgupta and B.R. Webber, Nucl. Phys. **B247**, 247 (1997); M. Beneke, V.M. Braun and L. Magnea, Nucl. Phys. **B497**, 297 (1997).

[29] P.J. Rijken and W.L. van Neerven, Nucl. Phys. **B487**, 233 (1997); Phys. Lett. **B386**, 422 (1996).

[30] M. Glück, E. Reya and A. Vogt, Z. Phys. **C48**, 471 (1990).

[31] M. Glück, E. Reya and A. Vogt, Z. Phys. **C53**, 127 (1992).

[32] M. Glück, E. Reya and A. Vogt, Phys. Lett. **B306**, 391 (1993).

[33] M. Glück, E. Reya and A. Vogt, Z. Phys. **C67**, 433 (1995).

[34] J. C. Collins and W.- K. Tung, Nucl. Phys. **B278**, 934 (1986). S. Qian, Argonne preprint ANL-HEP-PR-84-72, (*unpublished*).

[35] C. Caso *et al.*, Particle Data Group, Eur. Phys. J. **C3**, 1 (1998).

[36] M. Glück, E. Reya and A. Vogt, Phys. Rev. **D45**, 3986 (1992).

[37] A. Devoto and D.W. Duke, La Riv. Nuov. Cim. **7**, 1 (1984).

[38] J. Blümlein and S. Kurth, Phys. Rev. **D60**, 014018 (1999); J. Blümlein, DESY 98-149, `hep-ph/0003100`.

[39] E. Witten, Nucl. Phys. **B104**, 445 (1976); J.C. Collins, G. Sterman and D.E. Soper, Nucl. Phys. **B236**, 37 (1986); M. Glück, E. Reya and M. Stratmann, Nucl. Phys. **B422**, 37 (1994); M.A.G. Aivazis, J.C. Collins, F.I. Olness and W.- K. Tung, Phys. Rev. **D50**, 3102 (1994); J.C. Collins, Phys. Rev. **D58**. 094002 (1998); R.S. Thorne and R. G. Roberts, Phys. Rev. **D57**, 6871 (1998) ; R.S. Thorne and R. G. Roberts, Phys. Lett. **B421**, 303 (1998); M. Buza, Y. Matiounine, J. Smith, W.L. van Neerven, Eur. Phys. J. **C1**, 301 (1998); A.D. Martin, R.G. Roberts, M.G. Ryskin and W.J. Stirling, Eur. Phys. J. **C2**, 287 (1998); S. Kretzer, Phys. Lett. **B471**, 227-232 (1999).

[40] B. Mele and P. Nason, Nucl. Phys. **B361**, 626 (1991).

[41] M. Glück, E. Reya and M. Stratmann, Nucl. Phys. **B422**, 37 (1994).

[42] M. Cacciari and M. Greco, Phys. Rev. **D55**, 7134 (1997).

[43] P. Nason and C. Oleari, Phys. Lett. **B447**, 327 (1999).

[44] P. Nason and C. Oleari, Bicocca-FT-99-07, DTP/99/36, `hep-ph/9903541`.

[45] R. Akers *et al.*, OPAL Collab., Z. Phys. **C67**, 27 (1995).

[46] G. Hansper, Ph.D. thesis, Ruprecht-Karls-Universität Heidelberg, February 1998, HD-IHEP 98-03.

[47] P. Nason and C. Oleari, Nucl. Phys. **B521**, 237 (1998); G. Rodrigo, Nucl. Phys. Proc. Suppl. **54A**, 60 (1997); A. Brandenburg and P. Uwer, Nucl. Phys. **B515**, 279 (1998).

[48] K. Abe *et al.*, SLD Collab., Phys. Rev. **D56**, 5310 (1997).

[49] J. Dias de Deus and N. Sakai, Phys. Lett. **86B**, 321 (1979).

[50] K. Abe *et al.*, SLD Collab., Phys. Rev. Lett. **78**, 3442 (1997), **79**, 959 (1997) (E); G. Abbiendi *et al.*, OPAL Collab., CERN-EP/99-164, `hep-ex/0001054`.

[51] E. Reya, Phys. Rept. **69**, 195 (1981).

[52] `MINUIT`, CERN Computer Centre Program Library.

[53] J. Binnewies, Ph.D. Thesis, DESY 97-128, `hep-ph/9707269`.

[54] K. Ackerstaff *et al.*, OPAL Collab., Z. Phys. **C 75**, 193 (1997).

[55] D. Buskulic *et al.*, ALEPH Collab., Z. Phys. **C66**, 355 (1995).

[56] D. Buskulic *et al.*, ALEPH Collab., Phys. Lett. **B384**, 353 (1996); D. Barate *et al.*, ALEPH Collab., CERN-EP/98-16 (unpublished); P. Abreu *et al.*, DELPHI Collab., Z. Phys. **C70**, 179 (1996); Phys. Lett. **B401**, 118 (1997); Eur. Phys. J **C4**, 1 (1998); **C6**, 19 (1999); Phys. Lett. **B449**, 383 (1999); P.D. Acton *et al.*, OPAL Collab., Z.

Phys. **C58**, 387 (1993); K. Ackerstaff *et al.*, OPAL Collab., Eur. Phys. J. **C7**, 369 (1999).

[57] G. Abbiendi *et al.*, OPAL Collab., Eur. Phys. J. **C11**, 217 (1999).

[58] P. Abreu *et al.*, DELPHI Collab., CERN-EP/99-144.